ONIOM Study on a Missing Piece in Our Understanding of Heme Chemistry: Bacterial Tryptophan 2,3-Dioxygenase with Dual Oxidants

Lung Wa Chung,[†,‡] Xin Li,[†,‡] Hiroshi Sugimoto,[§] Yoshitsugu Shiro,[§] and Keiji Morokuma*,[†]

Fukui Institute for Fundamental Chemistry, Kyoto University, Kyoto 606-8103, Japan, and Biometal Science Laboratory, RIKEN SPring-8 Center, Harima Institute, Hyogo 679-5148, Japan
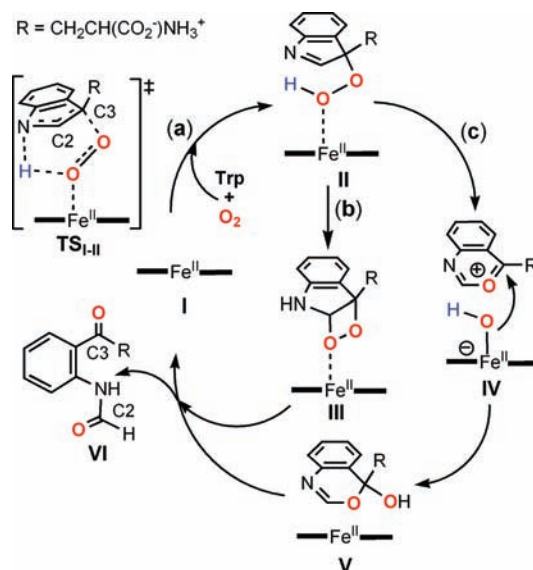
Received April 26, 2010; E-mail: morokuma@fukui.kyoto-u.ac.jp

Abstract: Unique heme-containing tryptophan 2,3-dioxygenase (TDO) and indoleamine 2,3-dioxygenase (IDO) catalyze oxidative cleavage of the pyrrole ring of L-tryptophan (Trp). Although these two heme dioxygenases were discovered more than 40 years ago, their reaction mechanisms were still poorly understood. Encouraged by recent X-ray crystal structures, new mechanistic pathways were proposed. We performed ONIOM(B3LYP:Amber) calculations with explicit consideration of the protein environment to study various possible reaction mechanisms for bacterial TDO. The ONIOM calculations do not support the proposed mechanisms (via either formation of the dioxetane intermediate or Criegee-type rearrangement); a mechanism that is exceptional in the hemes emerges. It starts with (1) direct radical addition of a ferric-superoxide intermediate with C2 of the indole of Trp, followed by (2) ring-closure via homolytic O−O cleavage to give epoxide and ferryl-oxo (Cpd II) intermediates, (3) acid-catalyzed regiospecific ring-opening of the epoxide, (4) oxo-attack, and (5) finally C−C bond cleavage concerted with back proton transfer. The involvement of dual oxidants, ferric-superoxide and ferryl-oxo (Cpd II) intermediates, is proposed to be responsible for the dioxygenase reactivity in bacterial TDO. In particular, the not-well-recognized ferric-superoxide porphyrin intermediate is found to be capable of reacting with π-systems via direct radical addition, an uncommon dioxygen activation in the hemes. The comparison between *Xanthomonas campestris* TDO and some heme as well non-heme oxygenases is also discussed.

1. Introduction

Tryptophan 2,3-dioxygenase (TDO) and indoleamine 2,3-dioxygenase (IDO) are unique heme-containing oxygenases which cleave the pyrrole ring of L-tryptophan (L-Trp) and insert both oxygen atoms of a dioxygen molecule into the substrate to afford *N*-formylkynurenine **VI** (Scheme 1).[1] This oxidative cleavage of Trp is the first and rate-limiting step in L-Trp catabolism through the kynurenine pathway.[2] Although TDO and IDO were discovered more than 40 years ago,[1] the reaction mechanism for these two heme-containing dioxygenases remains unclear. It is in sharp contrast with those for heme-containing monooxygenases (e.g., cytochrome P450, heme oxygenases (HO), and peroxidase) and non-heme dioxygenases (e.g., catechol dioxygenases and naphthalene dioxygenase).[1e,3,4] The missing reaction mechanism for TDO and IDO can be attributed to the fact that no proposed intermediates in TDO/IDO have been observed or characterized spectroscopically.

† Kyoto University.
§ RIKEN SPring-8 Center.
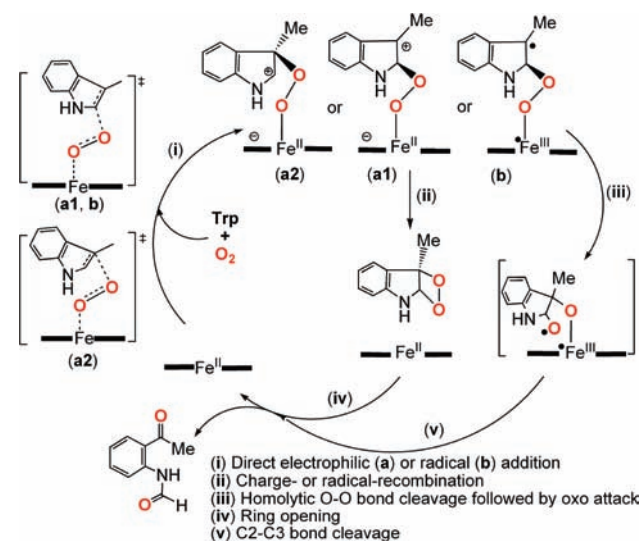‡ These authors contributed equally.

(1) (a) Kotake, Y.; Masayama, I. *Z. Physiol. Chem.* **1936**, *243*, 237. (b) Hayaishi, O.; Rothberg, S.; Mehler, A. H.; Saito, Y. *J. Biol. Chem.* **1957**, *229*, 889. (c) Yamamoto, S.; Hayaishi, O. *J. Biol. Chem.* **1967**, *242*, 5260. (d) Yoshida, R.; Hayaishi, O. *Methods Enzymol.* **1987**, *142*, 188. (e) Sono, M.; Roach, M. P.; Coulter, E. D.; Dawson, J. H. *Chem. Rev.* **1996**, *96*, 2841.
(2) Knox, W. E.; Mehler, A. H. *J. Biol. Chem.* **1950**, *187*, 419.

Scheme 1. Recently Proposed Pathways for IDO/TDO[a]

[a] Cf. refs 6a, 8, and 14a. These pathways are similar to the previous pathways (cf. ref 1e) except for the occurrence of proton (in blue) abstraction by an external base.

TDO is a homotetrameric enzyme that displays high substrate specificity and has been found in bacteria, mosquitoes, and the

liver and skin of mammals.[1e,5,6] In comparison, IDO is a monomeric enzyme that has a broader substrate specificity than TDO.[1e,7,8] Furthermore, IDO is ubiquitous in mammals except the liver and is also found to have monooxygenase activity.[9] The importance of IDO and TDO is related to a few important physiological functions, such as the suppression of T-cell proliferation, the syntheses of the neurotransmitter serotonin, nicotinamide adenine dinucleotide (NAD), and the hormone melatonin.[1e,10]

It has commonly been believed that the reactions of TDO and IDO start with deprotonation of the indole of Trp by a base, followed by an electrophilic addition of the ferrous-bound dioxygen intermediate to the C3 position of the resultant deprotonated Trp.[1e,11] However, the feasibility of this deprotonation step is controversial, as the intrinsic acidity of the indole is very low.[12] Remarkably, recent X-ray crystal structures of bacterial TDO and human IDO (hIDO) elucidated three-dimensional structures of the active sites for the first time, which significantly advances our understanding of this missing piece in heme chemistry.[6a,b,8,13] Although the sequence similarity between bacterial TDO and hIDO is very low, the active sites

Scheme 2. Our Proposed Mechanisms Derived from the Active-Site Model Calculations

(i) Direct electrophilic (**a**) or radical (**b**) addition
(ii) Charge- or radical-recombination
(iii) Homolytic O–O bond cleavage followed by oxo attack
(iv) Ring opening
(v) C2–C3 bond cleavage

are quite similar. In addition, their active sites are highly hydrophobic, and a hydrogen-bond network with bulk water solvent is absent in the distal pocket.[6a,8] Furthermore, site-directed mutagenesis studies showed that polar residues [e.g., His55 of *Xanthomonas campestris* TDO (xcTDO) and Ser167 of hIDO] in the active site do not play an important role in the enzymatic reaction.[6a,b,8] These features are in contrast to heme-containing monooxygenases, such as P450, peroxidase, HO, and nitric oxide synthase (NOS).[1e,3a,b,d,f,l]

Prompted by the recent experimental observations, two new mechanistic pathways starting with electrophilic addition of the ferrous-bound dioxygen coupled with proton transfer (i.e., concerted oxygen ene-type reaction) via TS_{I-II} followed by either formation of a dioxetane intermediate **III** (route b) or Criegee-type rearrangement (route c) were accordingly proposed (Scheme 1).[6a,b,8,13,14]

We previously performed density functional theory (DFT) calculations using an active-site model for the present system.[15] These calculations did not support the concerted but highly distorted transition state TS_{I-II}, as the calculated barrier is very high (27.0–40.3 kcal/mol) relative to the corresponding oxy-porphyrin-indole complexes. Instead, we proposed new dioxygen activation pathways involving direct electrophilic or radical addition *without deprotonation* for IDO and TDO (Scheme 2).[15] Moreover, our calculations denied the feasibility of the Criegee-type rearrangement from the neutral alkylperoxy intermediates (e.g., **II** in Scheme 1). Instead, after the direct additions, two competing mechanistic pathways were theoretically proposed: formation of the dioxetane intermediate via radical or charge recombination ((ii) in Scheme 2) or formation of the ferryl-oxo intermediate via homolytic O–O bond cleavage followed by oxo attack ((iii) in Scheme 2).[15] Very recently, Raven, Chapman, and co-workers demonstrated that 1-Me-L-Trp can be a substrate for hIDO (WT and S167A) as well as mutants of human TDO (hTDO: H76S) and xcTDO (H55A and H55S), albeit k_{cat} is

(3) (a) Rosen, G. M.; Tsai, P.; Pou, S. *Chem. Rev.* **2002**, *102*, 1191. (b) Colas, C.; Ortiz de Montellano, P. R. *Chem. Rev.* **2003**, *103*, 2305. (c) Costas, M.; Mehn, M. P.; Jensen, M. P.; Que, L., Jr. *Chem. Rev.* **2004**, *104*, 939. (d) Meunier, B.; de Visser, S. P.; Shaik, S. *Chem. Rev.* **2004**, *104*, 3947. (e) Abu-Omar, M. M.; Loaiza, A.; Hontzeas, N. *Chem. Rev.* **2005**, *105*, 2227. (f) Denisov, I. G.; Makris, T. M.; Sligar, S. G.; Schlichting, I. *Chem. Rev.* **2005**, *105*, 2253. (g) Shaik, S.; Kumar, D.; de Visser, S. P.; Altun, A.; Thiel, W. *Chem. Rev.* **2005**, *105*, 2279. (h) Poulos, T. L. *Biochem. Biophys. Res. Commun.* **2005**, *338*, 337. (i) *Ubiquitous Roles of Cytochrome P450 Proteins*; Sigel, A., Sigel, H., Sigel, R. K. O., Eds.; Metal Ions in Life Science *3*; John Wiley & Sons Ltd.: West Sussex, 2007. (j) Bugg, T. D. H. *Tetrahedron* **2003**, *59*, 7075. (k) Kovaleva, E. G.; Neibergall, M. B.; Chakrabarty, S.; Lipscomb, J. D. *Acc. Chem. Res.* **2007**, *40*, 475. (l) Matsui, T.; Unno, M.; Ikeda-Saito, M. *Acc. Chem. Res.* **2010**, *43*, 240. (m) Nam, W. *Acc. Chem. Res.* **2007**, *40*, 522. (n) Krebs, C.; Fujimori, D.; Walsh, C. T.; Bollinger, J. M., Jr. *Acc. Chem. Res.* **2007**, *40*, 484.
(4) (a) Borowski, T.; Siegbahn, P. E. M. *J. Am. Chem. Soc.* **2006**, *128*, 12941. (b) Borowski, T.; Georgiev, V.; Siegbahn, P. E. M. *J. Am. Chem. Soc.* **2005**, *127*, 17303. (c) Siegbahn, P. E. M.; Haeffner, F. *J. Am. Chem. Soc.* **2004**, *126*, 8919. (d) Siegbahn, P. E. M.; Borowski, T. *Acc. Chem. Res.* **2006**, *39*, 729. (e) Borowski, T.; Siegbahn, P. E. M. *Biochemistry* **2004**, *43*, 12331. (f) Aluri, S.; de Visser, S. P. *J. Am. Chem. Soc.* **2007**, *129*, 14846. (g) de Visser, S. P. *Coord. Chem. Rev.* **2009**, *253*, 754. (h) Bassan, A.; Blomberg, M. R. A.; Siegbahn, P. E. M. *J. Biol. Inorg. Chem.* **2004**, *9*, 439.
(5) Ishiguro, I.; Naito, J.; Saito, K.; Nagamura, Y. *FEBS Lett.* **1993**, *329*, 178.
(6) (a) Forouhar, E.; et al. *Proc. Natl. Acad. Sci. U.S.A.* **2007**, *104*, 473. (b) Thackray, S. J.; Bruckmann, C.; Anderson, J. L.; Campbell, L. P.; Xiao, R.; Zhao, L.; Mowat, C. G.; Forouhar, F.; Tong, L.; Chapman, S. K. *Biochemistry* **2008**, *47*, 10677. (c) Basran, J.; Rafice, S. A.; Chauhan, N.; Efimov, I.; Cheesman, M. R.; Ghamsari, L.; Raven, E. L. *Biochemistry* **2008**, *47*, 4752. (d) Rafice, S. A.; Chauhan, N.; Efimov, I.; Basran, J.; Raven, E. L. *Biochem. Soc. Trans.* **2009**, *37*, 408.
(7) Shimizu, T.; Nomiyama, S.; Hirata, F.; Hayaishi, O. *J. Biol. Chem.* **1978**, *253*, 4700.
(8) Sugimoto, H.; Oda, S.-I.; Otsuki, T.; Hino, T.; Yoshida, T.; Shiro, Y. *Proc. Natl. Acad. Sci. U.S.A.* **2006**, *103*, 2611.
(9) Benzphetamine demethylase and aniline hydroxylase activities: Takikawa, O.; Yoshida, R.; Hayaishi, O. *J. Biol. Chem.* **1983**, *258*, 6808.
(10) (a) Mellor, A. L.; Munn, D. H. *Nat. Rev. Immunol.* **2004**, *4*, 762. (b) Grohmann, U.; Fallarino, F.; Puccetti, P. *Trends Immunol.* **2003**, *24*, 242. (c) Uyttenhove, C.; Pilotte, L.; Theate, I.; Stroobant, V.; Colau, D.; Parmentier, N.; Boon, T.; van den Eynde, B. J. *Nat. Med.* **2003**, *9*, 1269. (d) Takikawa, O. *Biochem. Biophys. Res. Commun.* **2005**, *338*, 12. (e) Muller, A. J.; Scherle, P. A. *Nat. Rev. Cancer* **2006**, *6*, 613. (f) Katz, J. B.; Muller, A. J.; Prendergast, G. C. *Immunol. Rev.* **2008**, *222*, 206.
(11) Hamilton, G. A. *Adv. Enzymol.* **1967**, *32*, 55.
(12) Bordwell, F. G. *Acc. Chem. Res.* **1988**, *21*, 456.
(13) Zhang, Y.; Kang, S. A.; Mukherjee, T.; Bale, S.; Crane, B. R.; Begley, T. P.; Ealick, S. E. *Biochemistry* **2007**, *46*, 145.

(14) (a) Terentis, A. C.; Thomas, S. R.; Takikawa, O.; Littlejohn, T. K.; Truscott, R. J. W.; Armstrong, R. S.; Yeh, S.-R.; Stocker, R. *J. Biol. Chem.* **2002**, *277*, 15788. (b) Batabyal, D.; Yeh, S.-R. *J. Am. Chem. Soc.* **2007**, *129*, 15690. (c) Batabyal, D.; Yeh, S.-R. *J. Am. Chem. Soc.* **2009**, *131*, 3260.
(15) Chung, L. W.; Li, X.; Sugimoto, H.; Shiro, Y.; Morokuma, K. *J. Am. Chem. Soc.* **2008**, *130*, 12298.

reduced.[16] Therefore, deprotonation was shown not to be required in the reaction, which is in line with our proposed direct addition mechanisms (Scheme 2).[15]

Although recent studies on TDO and IDO have shed some new and important light on the protein structures, substrate recognition, and reactivity,[6a,b,8,13,14,16] the overall reaction mechanism at atomic resolution is still unclear.[17] To fill this gap, we performed quantum mechanics/molecular mechanics (QM/MM) calculations explicitly including the xcTDO protein into the calculation.[6a] Our QM/MM calculations show that the most favorable pathway for bacterial TDO (xcTDO) involves (a) direct radical addition of the ferric-superoxide intermediate to C2 of Trp, followed by (b) homolytic O—O cleavage concerted with ring-closure to give an epoxide and the ferryl-oxo (Cpd II) intermediates, (c) regiospecific ring-opening assisted by proton transfer of a nearby ammonium cation of the substrate itself, (d) oxygen-coupled electron transfer (OCET), and finally (e) C2—C3 bond cleavage concerted with back proton transfer. In addition, His55 is proposed to be capable of acting as an electrostatic catalyst via a hydrogen bond with the indole NH bond. Moreover, our proposed direct radical addition with the ferric-superoxide porphyrin intermediate may potentially be applied for other π-systems. Reaction mechanisms for xcTDO, common heme monooxygenases, and non-heme dioxygenases are also compared.

2. Computational Methods

2.1. System Preparation and Classical Calculations. The initial structure of xcTDO was obtained from the Protein Data Bank (PDB ID: 2NW8). Since the TDO active site is constructed from two monomers, both chains A and B as well as their surrounding crystal water molecules were adopted. Due to the poor quality of the C-terminal in chain B, some residues were missing in the crystal structure. As a result, we used residues $21-250$ of chain B and all the available residues $19-284$ of chain A.[18] The active site in chain A with higher quality was used to study the oxygenation reaction. The water molecule (WAT1) above the heme in the chain A was replaced by one dioxygen molecule, and manganese ions were deleted. Orientations of histidine, asparagine, and glutamine residues were examined by WhatCheck, MolProbity, and visual inspection to achieve better hydrogen-bonding or less steric repulsion.[19] Missing hydrogen atoms were added, and major hydrogen bond networks were optimized by the program PDB2PQR.[20a] Meanwhile, protonation states of the titratable residues at pH 7 were estimated by PROPKA implemented in PDB2PQR.[20] In addition, the protonation state of histidine, i.e., protonated at the δ or/and ε nitrogen, was decided from the local hydrogen-bonding network via visual inspection (see details in Supporting Information). The prepared structure was then fully solvated in the truncated octahedron water box constructed from a cubic box of 104.4 Å and neutralized by addition of five Na^+ counterions via the Amber Leap module.[21]

All classical molecular mechanics (MM) calculations have been performed with AMBER all-atom force field and TIP3P water model.[22] All available force field parameters, charges and atom types for all amino acids and oxy-heme were taken from the AMBER library. The water molecules and hydrogen atoms were first optimized, and then the entire system except the oxy-heme was further optimized to remove close contacts. A cutoff radius of 12 Å was used for nonbonding interactions, and electrostatic interactions were calculated with the Particle Mesh Ewald (PME)

method.[23] Finally, the solvation water molecules more than 5 Å away from the MM-optimized protein were removed for the initial geometry of the ONIOM optimizations. Thus, the entire system consists of 13235 atoms for our ONIOM(QM:MM) calculations (Scheme 3a).[24,25]

Besides the classical energy minimizations, a series of MM molecular dynamics (MD) simulations were also performed. Simulations of 50 ps duration in the temperature ranges of $0-100$, $100-200$, and then $200-300$ K under constant volume condition

(17) During the preparation of this manuscript, formation of the ferryl-oxo intermediate, which was proposed in our previous DFT calculations (cf. ref 15), in hIDO was independently observed by different groups through resonance Raman spectroscopy: (a) Yanagisawa, S.; Yotsuya, K.; Horitani, M.; Hashiwaki, Y.; Horitani, M.; Sugimoto, H.; Shiro, Y.; Appleman, E. H.; Ogura, T. *Chem. Lett.* **2010**, *39*, 36. (b) Lewis-Ballester, A.; Batabyal, D.; Egawa, T.; Lu, C.; Lin, Y.; Martib, M. A.; Capece, L.; Estrin, D. A.; Yeh, S.-R. *Proc. Natl. Acad. Sci. U.S.A.* **2009**, *106*, 17371. The preliminary QM/MM calculation for the first step was also published in ref 17b by Estrin and Yeh (EY). As to the mechanistic aspects, both QM/MM calculations independently suggested the addition at the C2 position first and finally give the epoxide and Cpd II. However, a concerted pathway was suggested in the previous QM/MM(PBE:Amber) calculations. On the other hand, from different starting structures, a stepwise pathway involving a Fe(III)-peroxy intermediate ^{3}2 was found in our ONIOM(B3LYP:Amber) calculations. Moreover, these two studies adopted a few different computational settings, and the key ones are listed as follows: (1) This work used chain A and most of the chain B; EY used most of chain A with a few residues of chain B. (2) In this work, additional TS structures and epoxidation TS structures were accurately determined by the recent TS optimization method and verified by frequency calculations; EY estimated the concerted addition—epoxidation TS structures by potential energy scan calculations along one of the reaction coordinates (O_d—C2 distance via stepwise increasing interval of 0.1 Å). (3) Based on the ONIOM(B3LYP: MM)-calculated reaction paths, we performed single-point calculations with PBE and Truhlar's M06 functionals (Table S3). Remarkably, PBE gave a negative activation barrier (-3.1 kcal/mol) for our epoxidation TS (^{3}TS$_{2-3}$), while B3LYP, B3LYP*, and M06 functional gave a positive activation barrier. That might result in the concerted mechanism in ref 17b. (c) PBE: Perdew, J. P.; Burke, K.; Ernzerhof, M. *Phys. Rev. Lett.* **1996**, *77*, 3865. (d) Perdew, J. P.; Burke, K.; Ernzerhof, M. *Phys. Rev. Lett.* **1997**, *78*, 1396. (e) M06: Zhao, Y.; Truhlar, D. G. *Theor. Chem. Acc.* **2008**, *120*, 215.

(18) (a) xcTDO is a tetramer protein, in which the active site is formed from the dimer. The shortest distances between the active site in chain A and residues in chain C: Glu224,11.8 Å; Val227, 12.9 Å; Thr231, 12.8 Å; Phe276, 11.9 Å; Arg279, 9.3 Å; Thr280, 11.3 Å; and Val282, 11.4 Å. To estimate the error of excluding these residues in chain C, we superimposed the X-ray crystal tetramer structure and the ONIOM-optimized reactant. We then took coordinates of these residues in chain C, added hydrogen atoms, and represented them as the point charges. Additional B3LYP calculations show negligible error of these electrostatic interactions (data in parentheses in column 12 of Table S3; maximum error of 0.2 kcal/mol). (b) ONIOM-calculated free energies are put in Table S3. More reliable QM/MM free energy calculations will be performed and reported in due course.

(19) (a) Hooft, R. W. W.; Vriend, G.; Sander, C.; Abola, E. E. *Nature* **1996**, *381*, 272. (b) Lovell, S. C.; Davis, I. W.; Arendall, W. B., III; de Bakker, P. I. W.; Word, J. M.; Prisant, M. G.; Richardson, J. S.; Richardson, D. C. *Proteins: Struct., Funct., Genet.* **2003**, *50*, 437.

(20) (a) Dolinsky, T. J.; Nielsen, J. E.; McCammon, J. A.; Baker, N. A. *Nucleic Acids Res.* **2004**, *32*, W665. (b) Li, H.; Robertson, A. D.; Jensen, J. H. *Proteins: Struct., Funct., Bioinf.* **2005**, *61*, 704.

(21) Case, D. A.; et al. *AMBER 9 and 10*; University of California: San Francisco, 2006 and 2008.

(22) (a) Cornell, W. D.; Cieplak, P.; Bayly, C. I.; Gould, I. R.; Merz, K. M.; Ferguson, D. M.; Spellmeyer, D. C.; Fox, T.; Caldwell, J. W.; Kollman, P. A. *J. Am. Chem. Soc.* **1995**, *117*, 5179. (b) Jorgensen, W. L.; Chandrasekhar, J.; Madura, J. D.; Impey, R. W.; Klein, M. L. *J. Comput. Phys.* **1983**, *79*, 926.

(23) (a) Darden, T.; York, D.; Pedersen, L. *J. Chem. Phys.* **1993**, *98*, 10089. (b) Essmann, U.; Perera, L.; Berkowitz, M. L.; Darden, T.; Lee, H.; Pedersen, L. G. *J. Chem. Phys.* **1995**, *103*, 8577.

(24) The optimized protein and its active site are similar to the X-ray crystal structure (Figure S1). The calculated RMSD is about 0.50 Å.

(25) Molecular graphs and animations were created by PyMOL: DeLano, W. L. The PyMOL Molecular Graphics System, 2002; http://www.pymol.org.

(16) Chauhan, N.; Thackray, S. J.; Rafice, S. A.; Eaton, G.; Lee, M.; Efimov, I.; Basran, J.; Jenkins, P. R.; Mowat, C. G.; Chapman, S. K.; Raven, E. L. *J. Am. Chem. Soc.* **2009**, *131*, 4186.

Scheme 3. (a, Left) Solvated xcTDO Protein and (b, Right) QM Models (Except Link Atoms) in Our ONIOM Calculations
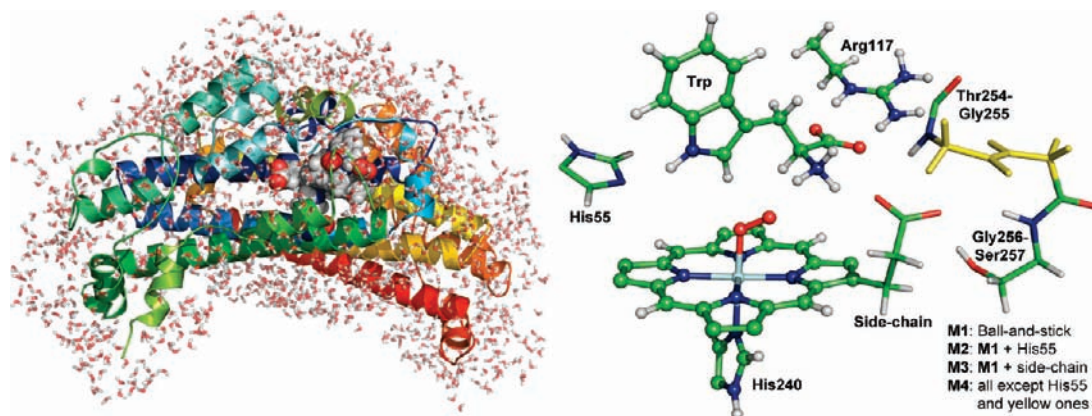
were performed to gradually heat the system. An additional 50 ps simulation in the NPT ensemble at 300 K and 1 bar was then performed, followed by 300 ps simulation in the NVT ensemble. Finally, a 10 ns MD simulation in the NVT ensemble representing the production run was carried out. The SHAKE algorithm was utilized to constrain all bond lengths involving hydrogen atoms.[26] The Leapfrog algorithm with a time step of 2 fs was used, and the temperature was controlled by the Langevin thermostat algorithm ($\gamma = 5$ ps^{-1}).[27] Four snapshots (1, 2, 3, and 5 ns) from the production run were adopted, in which solvation water molecules more than 5 Å away from the protein were removed, for ONIOM optimizations.

2.2. ONIOM(QM:MM) Calculations. A two-layer extrapolated (or so-called subtractive) QM/MM (i.e., ONIOM(QM:MM)) method was employed in this study,[28,29] in which the QM and MM parts were treated by the B3LYP[30] method and AMBER force field,[22] respectively. Basis sets 6-31G* were used for H, C, N, and O atoms. Hay and Wadt's effective core potentials (ECPs) and basis sets were adopted for the Fe atom.[31] This combination of the basis sets is labeled as BS1. The covalent boundary between the QM and MM regions is capped by hydrogen link atoms. To maintain integer MM charges for the QM model, the AMBER charges for the atoms near the QM/MM boundary were slightly adjusted. The whole system was further divided into the optimized MM region and the frozen MM region.[32] The residues within about 8 Å of the oxy-heme-indole were assigned to the optimized MM region and allowed to be optimized. As shown in Scheme 3b, the smallest QM model, M1 (91 atoms), consists of porphine, dioxygen, Trp, $CH_3CH_2CH_6N_3^+$, and imidazole as the truncated Arg117 and His240, respectively, for our ONIOM geometry optimization calculations (represented by a ball-and-stick model). All intermediates and transition states were optimized by an ONIOM mechanical embedding (ME) scheme. A new quadratic-coupled algorithm was used for transition-state optimization.[33,34] ONIOM harmonic vibrational frequency calculations at the same level were further performed to characterize and verify key transition states and intermediates.

As shown previously,[15] energies and geometries for the triplet state are generally similar to those for the open-shell singlet state (as two spins are separated). In addition, the previous DFT calculations showed that a triplet ferryl-oxo Cpd II intermediate is more stable than an open-shell ferryl-oxo intermediate, which was also found to have some spin contamination.[35] Therefore, geometry optimizations were mainly conducted in the triplet state (denoted by superscript 3), but geometry optimizations were also performed in closed-shell singlet, open-shell singlet, and quintet states for the key geometries (denoted by superscripts css, oss, and 5, respectively). Moreover, larger QM models (M2 and M4, see Scheme 3b) were employed for geometry optimizations of the very critical structures.

An ONIOM(QM:MM) electronic embedding (EE) scheme[36] was adopted for single-point energy calculations on the ONIOM-ME optimized structures (abbreviated as ONIOM-EE//ONIOM-ME). Apart from BS1, larger basis sets (BS2:6-311G* for H, C, N, and O atoms, as well as Stuttgart/Dresden ECP and basis sets augmented with f-polarization functions for Fe)[37] were used for the ONIOM-EE calculations. Recently, the parametrized B3LYP* was suggested to improve the energetics of different spin states for some iron complexes;[38] therefore, ONIOM(B3LYP*/BS2:Amber)-EE calculations were also carried out for the key cases. Moreover, several larger QM models, M3 and M4 in Scheme 3b, have been adopted in our ONIOM calculations with BS1 in order to examine QM effects of the nearby parts. All energies presented in the text are relative electronic energies mainly at the ONIOM(B3LYP/BS1:Amber)-ME level relative to the $^{oss}1$ unless otherwise stated.

(26) Ryckaert, J.-P.; Ciccotti, G.; Berendsen, H. J. C. *J. Comput. Phys.* **1977**, *23*, 327.

(27) (a) Pastor, R. W.; Brooks, B. R.; Szabo, A. *Mol. Phys.* **1988**, *65*, 1409. (b) Loncharich, R. J.; Brooks, B. R.; Pastor, R. W. *Biopolymers* **1992**, *32*, 523. (c) Izaguirre, J. A.; Catarello, D. P.; Wozniak, J. M.; Skeel, R. D. *J. Chem. Phys.* **2001**, *114*, 2090.

(28) (a) Maseras, F.; Morokuma, K. *J. Comput. Chem.* **1995**, *16*, 1170. (b) Humbel, S.; Sieber, S.; Morokuma, K. *J. Chem. Phys.* **1996**, *105*, 1959. (c) Matsubara, T.; Sieber, S.; Morokuma, K. *Int. J. Quantum Chem.* **1996**, *60*, 1101. (d) Svensson, M.; Humbel, S.; Froese, R. D. J.; Matsubara, T.; Sieber, S.; Morokuma, K. *J. Phys. Chem.* **1996**, *100*, 19357. (e) Svensson, M.; Humbel, S.; Morokuma, K. *J. Chem. Phys.* **1996**, *105*, 3654. (f) Dapprich, S.; Komáromi, I.; Byun, S.; Morokuma, K.; Frisch, M. J. *THEOCHEM* **1999**, *461*, 1. (g) Vreven, T.; Morokuma, K. *J. Comput. Chem.* **2000**, *21*, 1419.

(29) (a) Senn, H. M.; Thiel, W. *Angew. Chem., Int. Ed.* **2009**, *48*, 1198. (b) Senn, H. M.; Thiel, W. *Top. Curr. Chem.* **2007**, *268*, 173.

(30) (a) Becke, A. D. *J. Chem. Phys.* **1993**, *98*, 5648. (b) Lee, C.; Yang, W.; Parr, R. G. *Phys. Rev. B* **1988**, *37*, 785.

(31) Hay, P. J.; Wadt, W. R. *J. Chem. Phys.* **1985**, *82*, 299.

(32) Altun, A.; Shaik, S.; Thiel, W. *J. Comput. Chem.* **2006**, *27*, 1324.

(33) Vreven, T.; Frisch, M. J.; Kudin, K. N.; Schlegel, H. B.; Morokuma, K. *Mol. Phys.* **2006**, *104*, 701.

(34) Our previous ONIOM studies using this new algorithm: (a) Kwiecien, R. A.; Khavrutskii, I. V.; Musaev, D. G.; Morokuma, K.; Banerjee, R.; Paneth, P. *J. Am. Chem. Soc.* **2006**, *128*, 1287. (b) Li, X.; Chung, L. W.; Paneth, P.; Morokuma, K. *J. Am. Chem. Soc.* **2009**, *131*, 5115. (c) Prabhakar, R.; Vreven, T.; Frisch, M. J.; Morokuma, K.; Musaev, D. G. *J. Phys. Chem. B* **2006**, *110*, 13608. (d) Lundberg, M.; Kawatsu, T.; Vreven, T.; Frisch, M. J.; Morokuma, K. *J. Chem. Theory Comput.* **2009**, *5*, 222. (e) Hirao, H.; Morokuma, K. *J. Am. Chem. Soc.* **2009**, *131*, 17026.

(35) Derat, E.; Shaik, S. *J. Am. Chem. Soc.* **2006**, *128*, 8185.

(36) (a) Vreven, T.; Byun, K. S.; Komáromi, I.; Dapprich, S.; Montgomery, J. A., Jr.; Morokuma, K.; Frisch, M. J. *J. Chem. Theory Comput.* **2006**, *2*, 815. (b) Bakowies, D.; Thiel, W. *J. Phys. Chem.* **1996**, *100*, 10580.

(37) (a) Dolg, M.; Wedig, U.; Stoll, H.; Preuss, H. *J. Chem. Phys.* **1987**, *86*, 866. (b) Martin, J. M. L.; Sundermann, A. *J. Chem. Phys.* **2001**, *114*, 3408.

(38) (a) Reiher, M.; Salomon, O.; Hess, B. A. *Theor. Chem. Acc.* **2001**, *107*, 48. (b) Salomon, O.; Reiher, M.; Hess, B. A. *J. Chem. Phys.* **2002**, *117*, 4729. (c) Siegbahn, P. E. M. *J. Biol. Inorg. Chem.* **2006**, *11*, 695.
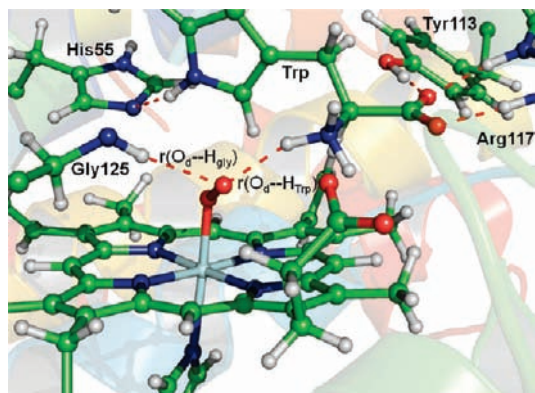
Figure 1. Most stable oxy-heme intermediate **1** for xcTDO calculated by the ONIOM(B3LYP/BS1:Amber) method. Only the key residues are shown for clarity.

2.3. QM Calculations. Besides the QM/MM calculations, a few additional calculations (geometry and frequency) have been performed at the B3LYP/BS1 level. Moreover, Mössbauer quadrupole splitting of the iron intermediates, which relates to the electric field gradient tensor at the nucleus, was calculated from $\Delta E_Q = 0.5eQV_{zz}(1 + \eta^2/3)^{0.5}$, where e is electron charge and Q is the quadrupole moment of ^{57}Fe in the $I^* = 3/2$ excited state;[39] 0.16 barn of Q[40] was commonly used for the theoretical calculations.[41] By convention, the principal components of the electric field gradient (EFG) tensors are defined as $|V_{zz}| > |V_{yy}| > |V_{xx}|$, and the asymmetry parameter $\eta = (V_{xx} - V_{yy})/V_{zz}$. The isomer shift can be estimated from $\delta_{Fe} = \alpha[\rho^{tot}(0) - c]$, where values of α and c (-0.404 and 11614.16, respectively) were calibrated against the experimental values of some iron complexes,[41b] and $\rho^{tot}(0)$ is the charge density at the nucleus. These calculations were performed by B3LYP with Wachter's basis sets for Fe, 6-311G* for the other heavy atoms, and 6-31G* for the hydrogen atom (denoted by BS3).[41,42] In addition, the fixed point charges of the MM part were embedded, and the Gaussian default scaling parameters for the boundaries were applied in the calculations.[36a] The charge density at the Fe nucleus was estimated by using the atoms-in-molecule (AIM) method.[43] All QM and ONIOM(QM:MM) calculations were carried out with Gaussian 03 and Gaussian Development Version program.[44]

3. Results and Discussion

3.1. Dioxygen Activation: Direct Additions. Our discussion of the reaction mechanism starts from oxy-heme intermediates (Figures 1 and 2 and Figure S2 in the Supporting Information, as well as Tables 1 and S1). Figure 1 shows the most stable form of the oxy-heme intermediate **1**, in which the distal oxygen (O_d) forms hydrogen bonds with an ammonium cation of the substrate (i.e., Trp) and the amide NH of Gly125. Similar to the other heme-containing oxygenases,[45,46] the open-shell singlet

(39) (a) Debrunner, P. G. In *Iron Porphyrins*; Lever, A. B. P., Gray, H. B., Eds.; VCH Publishers: New York, 1989; Vol. 3, pp 139−234. (b) Neese, F. *Coord. Chem. Rev.* **2009**, *253*, 526.
(40) Dufek, P.; Blaha, P.; Schwarz, K. *Phys. Rev. Lett.* **1995**, *75*, 3545.
(41) (a) Zhang, Y.; Mao, J.; Godbout, N.; Oldfield, E. *J. Am. Chem. Soc.* **2002**, *124*, 13921. (b) Zhang, Y.; Mao, J.; Godbout, N.; Oldfield, E. *J. Am. Chem. Soc.* **2002**, *124*, 7829. (c) Ling, Y.; Zhang, Y. *J. Am. Chem. Soc.* **2009**, *131*, 6386. (d) Sinnecker, S.; Slep, L. D.; Bill, E.; Neese, F. *Inorg. Chem.* **2005**, *44*, 2245.
(42) Wachters, A. J. *J. Chem. Phys.* **1970**, *52*, 1033.
(43) (a) Keith T. A. *AIMAll*, Version 09.04.23, 2009; aim.tkgristmill.com. (b) Bader, R. F. W. *Atoms in Molecules: A Quantum Theory*; Oxford University Press: Oxford, 1990.
(44) (a) Frisch, M. J.; et al. *Gaussian 03*, Revision C.02; Gaussian, Inc.: Wallingford, CT, 2004. (b) Frisch, M. J.; et al. *Gaussian Development*, Revisions G.01, G.03, and H.01; Gaussian, Inc.: Wallingford, CT, 2004.
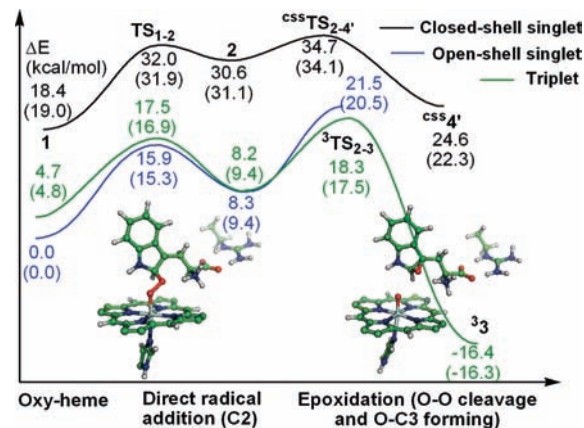
Figure 2. Potential energy profiles of the most favorable pathway for the first oxygen incorporation in xcTDO by the ONIOM(B3LYP/BS1:Amber) method. Energies with zero-point energy (ZPE) correction are in parentheses.

Table 1. Relative Energies (in kcal/mol), Key Structural Parameters (r, in Å), and Mulliken Spin Densities (s) of Oxy-heme Intermediate **1** Calculated by the ONIOM(B3LYP/BS1:Amber) Method

	css**1**	oss**1**	³**1**
$\Delta E_{ONIOM-ME}$	18.4	0.0	4.7
$\Delta E_{ONIOM-EE}$[a]	18.5	0.0	4.7
$r(Fe-O_p)$	1.74	1.90	1.92/1.91[b]
$r(O_p-O_d)$	1.28	1.29	1.30/1.29[b]
$r(O_d \cdots H_{Trp})$	2.22	2.08	1.90/1.91[b]
$r(O_d \cdots H_{gly})$	2.24	2.29	2.41/2.43[b]
$s(Fe)$		1.25	1.08/1.07[b]
$s(O_p)$		−0.53	0.41/0.42[b]
$s(O_d)$		−0.65	0.54/0.54[b]
$s(por)$		−0.07	−0.02/−0.02[b]

[a] ONIOM(B3LYP/BS1:Amber)-EE//ONIOM(B3LYP/BS1:Amber)-ME. [b] Data obtained by using model M2.

ferric-superoxide intermediate (oss**1**) is the most stable form, lower in energy than that in the triplet state (³**1**) and the ferrous-dioxygen intermediate in the closed-shell singlet state (css**1**) by 4.7 and 18.4 kcal/mol, respectively (Table 1).[47] The ferric-superoxide form is unambiguously supported by the calculated spin density; one spin is located on the iron, and the other spin is delocalized on the oxygen atoms. As shown recently,[45a] the ferric-superoxide state cannot be conclusively assigned by the calculated bond distances and charges.[17b] The ferric-superoxide state is also consistent with very recent studies.[17] Because there is more charge transfer from Fe to O_2 in oss,³**1** than css**1**, the distal oxygen (O_d) can form a stronger hydrogen bond with the ammonium cation (HN^+_{Trp}) of Trp (Table 1) in the former states than in the latter state.[48]

As proposed previously,[15] direct radical addition transition states ossTS$_{1-2}$ and ³TS$_{1-2}$ from the ferric-superoxide heme intermediates oss**1** and ³**1**, respectively (formal 1e transfer from Trp, eq 1), and direct electrophilic addition transition state

(45) (a) Wang, D.; Thiel, W. *THEOCHEM* **2009**, *898*, 90. (b) Nakashima, H.; Hasegawa, J.-Y.; Nakatsuji, H. *J. Comput. Chem.* **2006**, *27*, 426. (c) Blomberg, L. M.; Blomberg, M. R. A.; Siegbahn, P. E. M. *J. Inorg. Biochem.* **2005**, *99*, 949. (d) Rydberg, P.; Sigfridsson, E.; Ryde, U. *J. Biol. Inorg. Chem.* **2004**, *9*, 203.
(46) Chen, H.; Ikeda-Saito, M.; Shaik, S. *J. Am. Chem. Soc.* **2008**, *130*, 14778.
(47) The relative stability of **1** in different states is essentially unchanged when the ONIOM-EE method, changing the basis sets, or changing the functional is used (Tables 1 and 2).
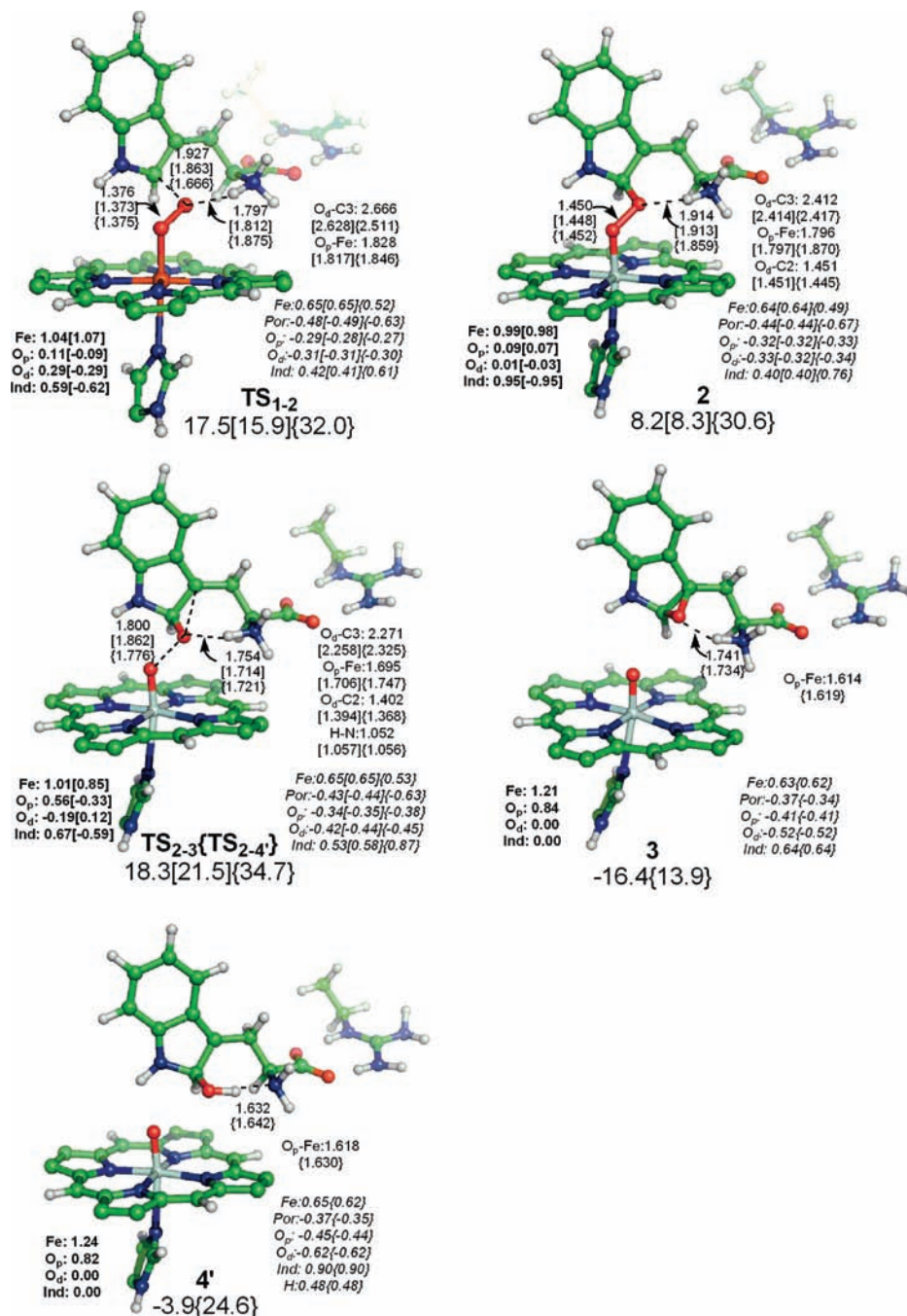
Figure 3. Calculated key structural parameters and relative energies (in kcal/mol) for the first oxygen incorporation processes. Bond lengths (Å), Mulliken charges, and spin densities are in plain, italic, and bold fonts, respectively. Values obtained from triplet, open-shell singlet (in square brackets), and closed-shell singlet (in curly brackets) are given.

^{css}TS$_{1-2}$ from the ferrous-dioxygen heme intermediate ^{css}1 (formal 2e transfer from Trp, eq 2) in xcTDO were located and characterized by the ONIOM calculations (Figures 2, 3, and S3 and Movie S1).

---

(48) (a) Conformers ^{css}1′ and ^{3}1′, in which the distal oxygen points away from the ammonium cation and forms weaker hydrogen bonds with the amide NH of Gly125, were calculated to be less stable than ^{css}1 and ^{3}1 by about 1.1 and 2.6 kcal/mol, respectively (Figure S2 and Table S1). (b) Another conformer, ^{css}1″, with the distal oxygen forming a hydrogen bond with the ammonium cation was calculated to be less stable than ^{css}1 by 0.4 kcal/mol by the ONIOM-ME method (Figure S2 and Table S1). However, the relative stability of ^{css}1″ is further decreased to 1.2−1.3 kcal/mol by the ONIOM-EE//ONIOM-ME method, irrespective of using larger basis set BS2 or B3LYP* functional.
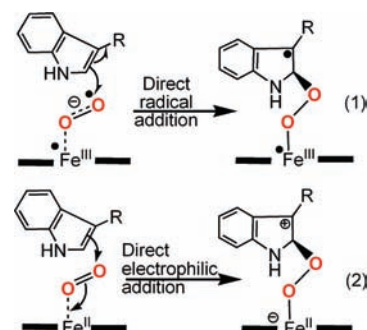
Table 2. Calculated Relative Energies of Key Intermediates and Transition States with Different Basis Sets (BS1 and BS2), Electronic Embedding (EE), Functionals (B3LYP and B3LYP*), and QM Models (M1, M3, and M4) Based on the ONIOM(B3LYP/BS1:Amber)-ME Optimized Structures

	model					
	M1, ME[a]	M1, EE[a]			M3, EE[a]	M4, ME[a]
	BS1	BS1	BS2	B3LYP*/BS2	BS1	BS1
³1	4.7	4.7	4.5	4.5	4.7	5.3
³TS$_{1-2}$	17.5	18.7	20.1	18.5	16.9	18.6
³2	8.2	10.0	13.0	12.4	8.3	8.2
³TS$_{2-3}$	18.3	20.4	22.9	18.7	19.1	19.5
³3	−16.4	−13.6	−11.5	−14.4	−14.7	−15.5
³TS$_{3-4}$	−8.9	−1.3	−1.2	−4.7	−1.9	−1.5
³4	−12.7	1.4	0.2	−2.8	1.3	0.8/−9.8[b]
³TS$_{4-5}$	−5.4	6.2	4.6	0.7	5.8	8.4
³5	−23.1	−9.6	−9.4	−10.2	−10.3	−8.2
³TS$_{5-P}$	−18.5	−6.2	−6.6	−7.8	−6.8	−5.4

[a] ME and EE stand for mechanical embedding and electronic embedding schemes applied in the calculations. The B3LYP functional was used in all calculations unless B3LYP* is stated. [b] The relative QM energy of −7.2 kcal/mol based on optimization with the ONIOM-(B3LYP/BS1:MM) ME method and model M4.

The O_d attacks the C2 position of the indole moiety of Trp in ^{css,oss,3}TS$_{1-2}$, rather than the widely accepted C3 position. The calculated barrier of the direct addition via ^{css,oss,3}TS$_{1-2}$ relative to the corresponding oxy-heme complex ^{css,oss,3}1 is 13.6, 15.9, and 12.8 kcal/mol, respectively. Since ferric-superoxide intermediates ^{oss,3}1 are energetically more stable than ^{css}1,[45,46] the direct radical addition is kinetically more favorable than the direct electrophilic addition (Figure 2). Such kinetic and thermodynamic preferences for the direct radical addition are not changed by using the ONIOM-EE scheme, larger basis sets, or the B3LYP* functional (Tables 2 and S2). It should be noted that such a direct addition mechanism involving the ferric-superoxide intermediate is quite exceptional in heme-containing oxygenases,[3,49−52] although a ferric-superoxide intermediate was found or proposed to play an active role in non-heme systems.[3c,e,k,34d,e,53] The direct radical addition leads to diradical intermediates ^{oss}2 and ^{3}2 having essentially the same stability,[54] while the direct electrophilic addition leads to a less stable zwitterionic intermediate, ^{css}2 (Figures 2 and 3 and eqs 1 and 2). Importantly, the direct radical addition transition state ^{3}TS$_{1-2}$ and product ^{3}2 can also be located starting from four different MD snapshots having similar structures and energies (Figure S4).

Attempts to locate transition states and products via direct addition at the C3 position (Scheme 2) from several different starting structures were unsuccessful. Instead, the calculations for the direct addition product directly led to the metastable dioxetane intermediates (^{css,3}DO), which are more stable than ^{css,3}1 by 11.9−13.4 kcal/mol (Figure S6 and Table S2). It should be noted that C3 is positioned farther away from the reacting O_d than C2 in the X-ray crystal structure, MD simulations (Figure S5), and ONIOM calculations. Unlike in the gas phase (Figure S7),[15] C3 cannot freely come close to the distal oxygen in xcTDO, even by slightly sloping the indole plane. In addition, when the indole moiety moves toward the heme plane and the Fe−O_p single bond remains intact, the indole is in too-close contact with the heme plane (i.e., steric repulsion, cf. Figure S7). Therefore, the protein environment in xcTDO is suggested to choose only one of the direct addition modes (C2), the energetically most favorable one in the gas phase,[15] which dictates the subsequent reaction pathway along with the formation of the unexpected epoxide and ferryl-oxo intermediates (see below).[55]

3.2. Epoxidation. Since the proximal oxygen (O_p) is *trans* to the C3 of the indole moiety in ^{css,oss,3}2, the formation of the metastable dioxetane intermediates (^{css,3}DO, Schemes 1 and 2), found previously in the active-site model in the gas phase,[15] requires significant rotation of the indole ring of Trp, which is impossible in the protein.[56] Instead, ^{oss,3}2 and ^{css}2 were found to undergo homolytic and heterolytic O−O bond cleavage[57] via ^{oss,3}TS$_{2-3}$ and ^{css}TS$_{2-4'}$, respectively. The frequency calculations and full optimization from the lowest-energy transition state ^{3}TS$_{2-3}$ show that homolytic O−O cleavage takes place with simultaneous O_d−C3 bond formation to give the unanticipated epoxide and ferryl-oxo intermediates (Cpd II) (see Movie S2).[17,58] The calculated barrier for this epoxidation process relative to ^{oss,3}2 is about 10.1 and 13.2 kcal/mol for triplet and open-shell singlet states, respectively (Figure 2). On the other hand, heterolytic O−O cleavage via ^{css}TS$_{2-4'}$ was found to couple with proton transfer from the ammonium cation of Trp and give an intermediate, ^{css}4′, in the closed-shell singlet state (Scheme 4). This heterolytic O−O cleavage process via ^{css}TS$_{2-4'}$ was calculated to be higher in energy than ^{3}TS$_{2-3}$ by 16.4 kcal/

(49) Ferric-superoxide heme intermediate was also proposed to be involved in nitric oxide dioxygenase (NOD): (a) Gardner, P. R.; Gardner, A. M.; Martin, L. A.; Salzman, A. L. *Proc. Natl. Acad. Sci. U.S.A.* **1998**, *95*, 10378. (b) Blomberg, L. M.; Blomberg, M. R. A.; Siegbahn, P. E. M. *J. Biol. Inorg. Chem.* **2004**, *9*, 923. (c) Schopfer, M. P.; Mondal, B.; Lee, D.-H.; Sarjeant, A. A. N.; Karlin, K. D. *Am. Chem. Soc.* **2009**, *131*, 11304.

(50) Unusual proposed mechanism for oxidative cleavage of indole: Lara, M.; Mutti, F. G.; Glueck, S. M.; Kroutil, W. *J. Am. Chem. Soc.* **2009**, *131*, 5368.

(51) HO: (a) Kamachi, T.; Shestakov, A. F.; Yoshizawa, K. *J. Am. Chem. Soc.* **2004**, *126*, 3672. (b) Sharma, P. K.; Kevorkiants, R.; de Visser, S. P.; Kumar, D.; Shaik, S. *Angew. Chem., Int. Ed.* **2004**, *43*, 1129. (c) Kumar, D.; de Visser, S. P.; Shaik, S. *J. Am. Chem. Soc.* **2005**, *127*, 8204. (d) Kamachi, T.; Yoshizawa, K. *J. Am. Chem. Soc.* **2005**, *127*, 10686. Aromatase: (e) Hackett, J. C.; Brueggemeier, R. W.; Hadad, C. M. *J. Am. Chem. Soc.* **2005**, *127*, 5224.

(52) NOS: (a) Cho, K.-B.; Gauld, J. W. *J. Am. Chem. Soc.* **2004**, *126*, 10267. (b) Cho, K.-B.; Gauld, J. W. *J. Phys. Chem. B* **2005**, *109*, 23706. (c) Robinet, J. J.; Cho, K.-B.; Gauld, J. W. *J. Am. Chem. Soc.* **2008**, *130*, 3328. (d) Cho, K.-B.; Derat, E.; Shaik, S. *J. Am. Chem. Soc.* **2007**, *129*, 3182. (e) de Visser, S. P.; Tan, L. S. *J. Am. Chem. Soc.* **2008**, *130*, 12961. (f) Cho, K.-B.; Carvajal, M. A.; Shaik, S. *J. Phys. Chem. B* **2009**, *113*, 336.

(53) (a) Bollinger, J. M., Jr.; Krebs, C. *Curr. Opin. Chem. Biol.* **2007**, *111*, 151. (b) Bollinger, J. M., Jr.; Diao, Y.; Matthews, M. L.; Xing, G.; Krebs, C. *Dalton Trans.* **2009**, 905.

(54) The relative energy of the optimized ^{3}2, ^{3}3, ^{3}4 and ^{3}4′ in the quintet state is 22.6, 2.7, 6.6, and 15.4 kcal/mol, respectively. The relative energy of the optimized ^{5}3 and ^{5}4 in the quintet state is −1.7 and 2.2 kcal/mol, respectively. Compared to the triplet state, the higher-energy quintet state should be unimportant in the reactions.

(55) Other possible dioxygen activation pathways were also examined, but they were found to be less feasible than the direct radical addition (Scheme S1 and Figures S6 and S8). For instance, PCET process, in which one proton was transferred from the ammonium cation and an electron is transferred partly from the indole part of the Trp and porphyrin, leads to an unstable hydroperoxy product ^{3}8. O−O bond cleavage from this hydroperoxy intermediate (heme-oxygenase type reaction) was computed to be much higher in energy (Figures S8 and S9) than the most favorable pathway (Figure 2). On the other hand, attempts to form a ferric-peroxy anion intermediate via electron transfer from the Trp to the ferric-superoxide intermediate were unsuccessful, presumably due to low electron affinity of the superoxide moiety.

(56) Alternatively, ^{3}2 could proceed homolytic Fe−O_p bond cleavage, followed by rotation of the C2−O_d bond and finally radical recombination to afford the metastable dioxetane intermediates ^{3}DO. However, the energy to elongate the Fe−O_p bond from ^{3}2 is computed to be higher than that of ^{3}TS$_{2-3}$ (Figure S10).

(57) Chen, H.; Hirao, H.; Derat, E.; Schlichting, I.; Shaik, S. *J. Phys. Chem. B* **2008**, *112*, 9490.

Scheme 4. Heterolytic O−O Bond Cleavage Coupled with Proton Transfer
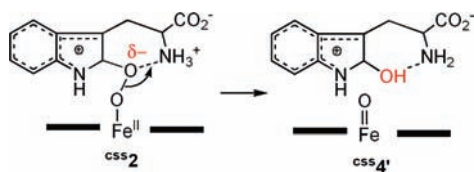
mol. As in our previous gas-phase work,[15] we could not locate the Criegee-type rearrangement transition state from the neutral alkylperoxy intermediates ^{3}**2**, likely due to the higher barrier and unstable resultant product.[15,59] In contrast to our current study, one recent preliminary QM/MM calculations suggested direct epoxidation from **1**.[17b] As found in one non-heme dioxygenase,[60] the possibility of direct epoxidation (when the distal oxygen could come close to both the C2 and C3 concurrently) cannot be completely ruled out. Two mechanistic pathways (i.e., direct addition followed by epoxidation or direct epoxidation) might be competitive and influenced by the dynamic position of the Trp with respect to the distal oxygen, although the Trp was not found to alter its conformation (e.g., RMSF = 0.56 Å, Figure S5) and change relative position considerably in our 10-ns MD simulations. Thus, we favor the former pathway in xcTDO.

3.3. Acid-Catalyzed Regiospecific Ring-Opening. Epoxides are relatively stable, and so a high activation energy or a catalytic acid or base may be required for the ring-opening. Very interestingly, xcTDO modulates the conformation and position of Trp so that its ammonium cation is perfectly positioned near the epoxide oxygen (O_d···H_{Trp} = 1.74 Å). Two isomeric ring-opening transition states from the epoxide ^{3}**3** were located and found to be driven by proton transfer from the nearby ammonium cation of the substrate itself (Figures 4 and 5). Ring-opening transition state ^{3}**TS$_{3-4}$**, leading to intermediate ^{3}**4** upon the C2−O_d bond breaking (Figure 4), is lower in energy than another transition state, ^{3}**TS$_{3-4'}$**, giving ^{3}**4'**, by 8.6 kcal/mol (Scheme 5). This is apparently due to the higher stability of ^{3}**4** than ^{3}**4'**, since the formal cation on the C2 in ^{3}**4** can be stabilized by the adjacent nitrogen lone-pair. Ring-opening of transition states ^{css}**TS$_{3-P}$** and ^{3}**TS$_{3-7}$**, which involves C2−C3 bond cleavage to give the final product ^{css}**P** and intermediate ^{3}**7**, respectively, without the aid of a proton transfer, was computed to have much higher barriers (26.6−35.3 kcal/mol relative to ^{css,3}**4**, see Figures 4, 5, S3, and S4 and Scheme 5). Interestingly, the oxo ligand was found to attack the C2 position during the C2−C3 bond cleavage in ^{css}**TS$_{3-P}$** and ^{3}**TS$_{3-7}$**. Therefore, these calculations suggest that proton transfer from the substrate itself should be critical for the subsequent reactions to give the dioxygenase product **P**.[61] Otherwise, the epoxide (the monooxygenase product) may be formed. Recently, the ferryl-oxo ligand was
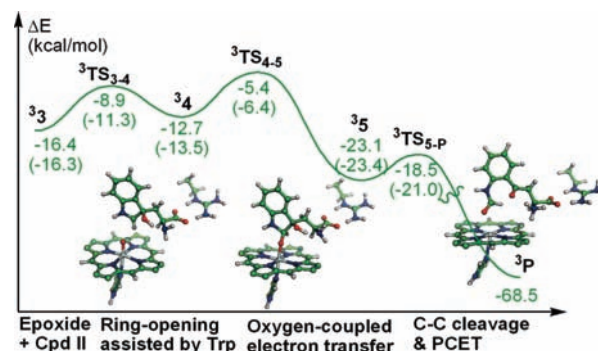
Figure 4. Potential energy profiles for the second oxygen incorporation processes in the triplet state in xcTDO by the ONIOM(B3LYP/BS1:Amber) method. Energies with ZPE correction are in parentheses.

suggested to be basic in chloroperoxidase (CPO).[62] Therefore, we also studied the possibility of proton transfer from the hydroxyl group in the stable intermediate ^{3}**4** to the oxo ligand. However, we could not locate a transition state for this transformation, due to its remote distance (O···O = 3.70 Å), and the resultant product ^{3}**4''** was found to be less stable than ^{3}**4** (Scheme 6). On the basis of the spin population, this process is not simple proton transfer (Figure S6) but rather proton-coupled electron transfer (PCET) to the oxo ligand, in which an electron is transferred partly from both Trp and porphyrin.

3.4. Oxygen-Coupled Electron-Transfer (Oxo Attack). After the acid-catalyzed regiospecific ring-opening of the epoxide via ^{3}**TS$_{3-4}$** takes place, the oxo ligand attacks the coordinately unsaturated C2 of the indole moiety to give intermediate ^{3}**5**. The oxo-attack transition state ^{3}**TS$_{4-5}$** was located slightly higher in energy than ^{3}**TS$_{3-4}$**, by 3.5 kcal/mol (Figure 4). Most of the spin density still resides on the ferryl center in ^{3}**TS$_{4-5}$**. Upon full optimization from ^{3}**TS$_{4-5}$** to ^{3}**5**, one-electron transfer from the electron-rich indole moiety to the iron takes place along with Fe−O_p bond elongation (1.868 Å, a single Fe−O bond) in ^{3}**5** (Scheme 7 and Figure 5). We could not locate an intermediate with Fe=O bond character; only electromer ^{3}**5** was found,[35] partly to relieve the steric repulsion between the C2H of the indole moiety and heme (cf. Figure S7). The overall process is analogous to oxygen-coupled electron transfer (OCET) theoretically observed in NOS.[52f]

3.5. C−C Cleavage. To complete the entire reaction in TDO, intermediate ^{3}**5**, which has a quite weak C2−C3 bond (1.625 Å), has to undergo C2−C3 bond cleavage via ^{3}**TS$_{5-P}$**, with a very small barrier of about 4.6 kcal/mol, or 2.4 kcal/mol if ZPE correction is included (Figure 4). The frequency calculations and full optimization from ^{3}**TS$_{5-P}$** toward the product side show that C−C bond cleavage is coupled with back proton transfer (Movie S5). Alternatively, another transition state, ^{3}**TS$_{5-6}$**,

(58) Homolytic cleavage of the O−O bond from Fe(III)-alkylperoxo intermediates to give ferryl-oxo intermediates: (a) Kojima, T.; Leising, R. A.; Yan, S.; Que, L., Jr. *J. Am. Chem. Soc.* **1993**, *115*, 11328. (b) Kim, J.; Harrison, R. G.; Kim, C.; Que, L., Jr. *J. Am. Chem. Soc.* **1996**, *118*, 4373. (c) Lehnert, N.; Ho, R. Y. N.; Que, L., Jr.; Solomon, E. I. *J. Am. Chem. Soc.* **2001**, *123*, 8271. (d) Bassan, A.; Blomberg, M. R. A.; Siegbahn, P. E. M.; Que, L., Jr. *J. Am. Chem. Soc.* **2002**, *124*, 11056. (e) Kryatov, S. V.; Rybak-Akimova, E. V.; Schindler, S. *Chem. Rev.* **2005**, *105*, 2175.

(59) In the gas-phase calculation, only the ring-closure transition state, but not the Criegee-type rearrangement transition state, was located for the simple radical hydroperoxy intermediate (Figure S11).

(60) Borowski, T.; Blomberg, M. R. A.; Siegbahn, P. E. M. *Chem.−Eur. J.* **2008**, *14*, 2264.

(61) One reviewer raised the possibility of conversion of the epoxide to the product involving hydrogen atom abstraction from the indole. Attempts to transfer H from the indole to His55 failed, but the optimization led back to the indole (see section 3.6). The ferryl-oxo could abstract hydrogen atom from the indole followed by hydroxyl attack (Figure S20 in ref 15), but it loses hydrogen-bonding between the indole and conserved His55 and changes orientation of the indole plane (cf. ^{3}**IV** in Figure S17) in the protein. Moreover, the recent experiment using *N*-methyl-Trp as the substrate showed that proton or hydrogen transfer from the indole is not necessary.[16]

(62) (a) Green, M. T.; Dawson, J. H.; Gray, H. B. *Science* **2004**, *304*, 1653. (b) Stone, K. L.; Behan, R. K.; Green, M. T. *Proc. Natl. Acad. Sci. U.S.A.* **2006**, *103*, 12307. (c) Stone, K. L.; Hoffart, L. M.; Behan, R. K.; Krebs, C.; Green, M. T. *J. Am. Chem. Soc.* **2006**, *128*, 6147. (d) Lai, W.; Chen, H.; Shaik, S. *J. Phys. Chem. B* **2009**, *113*, 7912.
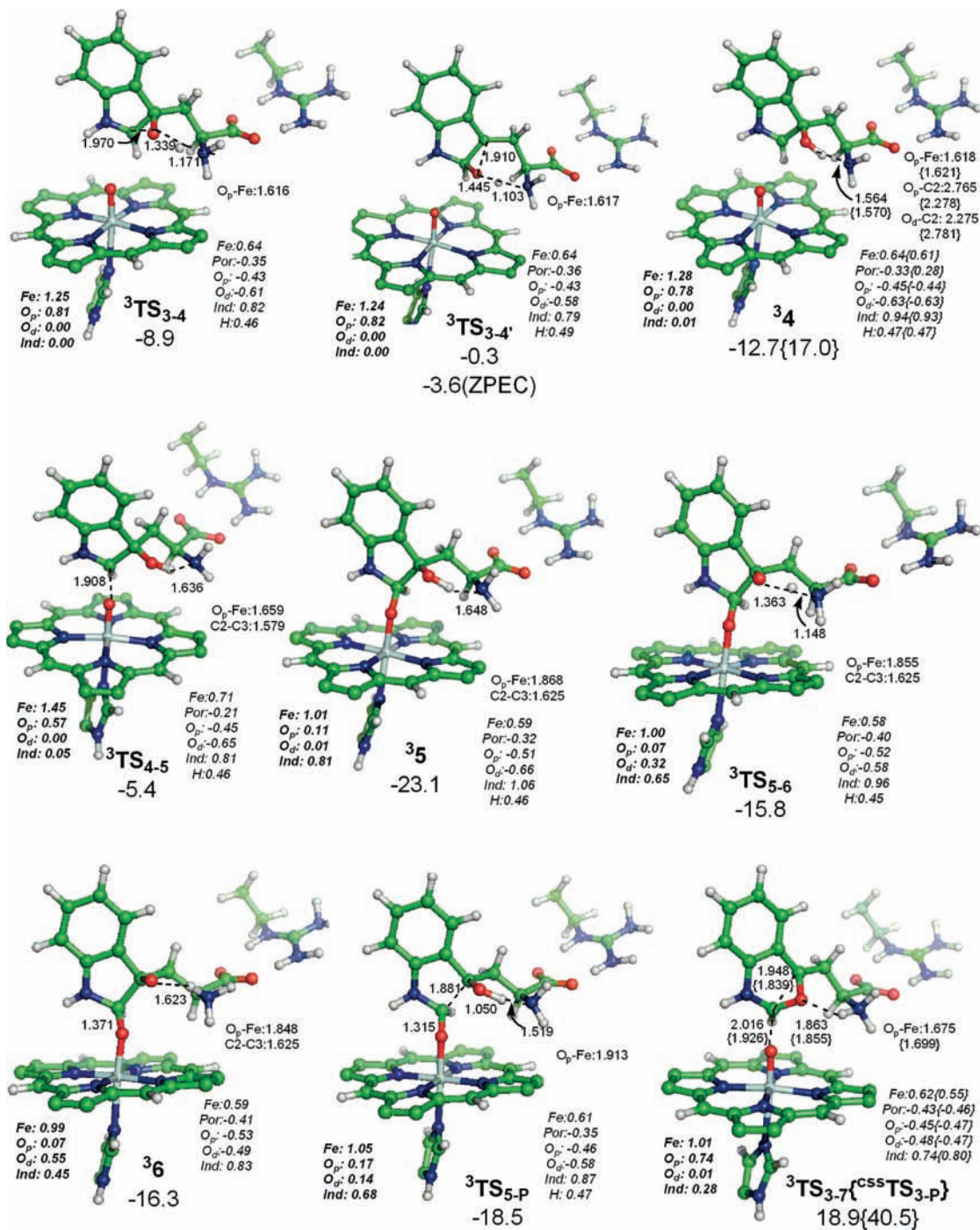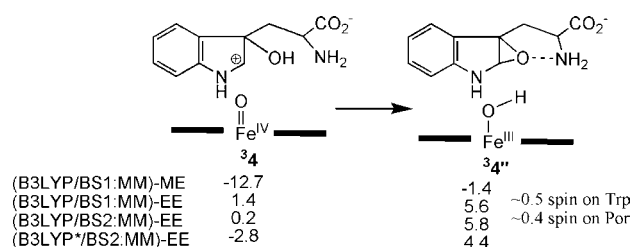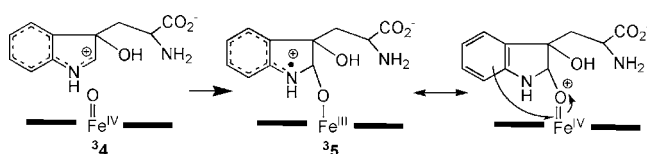
Figure 5. Calculated key structural parameters and relative energies (in kcal/mol) for the ring-opening, oxygen-coupled electron-transfer, and C−C bond cleavage processes. Bond lengths (Å), Mulliken charges, and spin densities are in plain, italic, and bold fonts, respectively. Values obtained from triplet, open-shell singlet (in square brackets), and closed-shell singlet (in braces) are given.

Scheme 5. Relative Energies (kcal/mol) for the Less Favorable Ring-Opening Processes
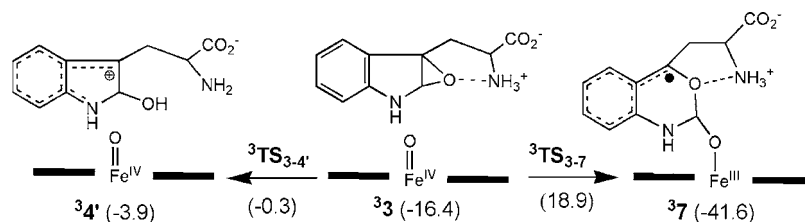
containing some PCET character, was found to give an alkoxy radical intermediate, **³6** (Figure 5). Unfortunately, we failed to

locate the subsequent C−C cleavage transition state from **³6**. The relaxed scan calculations along the C2−C3 bond suggest

Scheme 6. Relative Energies (kcal/mol) for PCET

(B3LYP/BS1:MM)-ME	-12.7
(B3LYP/BS1:MM)-EE	1.4
(B3LYP/BS2:MM)-EE	0.2
(B3LYP*/BS2:MM)-EE	-2.8

-1.4	
5.6	~0.5 spin on Trp
5.8	~0.4 spin on Por
4.4	

Scheme 7. Schematic Diagram for the Oxo Attack (Oxygen-Coupled Electron Transfer)

that this process is essentially barrierless (Figure S12). Therefore, these two pathways involving C2−C3 bond cleavage and proton transfer via $^3TS_{5-P}$ and $^3TS_{5-6}$, which demand a very low barrier, could be considered as concerted but asynchronous.[63] As previously discussed, another C−C cleavage process from the epoxide intermediate ^{33} via $^3TS_{3-7}$ was found without the acid catalyst but was much higher in energy (Figure 5).

3.6. Possible Roles of His55. The role of the conserved His55 (His76 in hTDO), which forms a hydrogen bond with the indole of Trp in xcTDO (Figure 1), is not clear and is under debate, although His55 was proposed to act as the putative catalytic base to deprotonate the indole.[14b,c] However, mutation of His55 does not kill the reactivity, particularly when N-methyl Trp is used.[6a,16] The recent crystal structures of wild-type and mutants of xcTDO (H55A and H55S) show that the Trp substrate moves away from the heme center but closer to residue 55 in these two mutants.[6a,b] Therefore, His55 was proposed to regulate substrate binding for the oxidative reaction (substrate preorganization) and suppress the formation of the nonproductive ferric substrate.[6b]

The feasibility of deprotonation of the weakly acidic indole by the conserved His55 was also examined by using the QM model M2. All attempts to optimize intermediates containing the protonated His55 and deprotontated indole moiety from intermediates $^{css}2$, ^{34}, $^34'$, and ^{35} were unsuccessful. The ONIOM optimizations spontaneously undergo back proton transfer to give the neutral His55 and neutral indole moiety. This is apparently because of the low acidity of the indole as well as the low basicity of the imidazole. Alternatively, since the ONIOM calculations suggest that the indole can participate in electron transfer in some of the catalytic steps, His55 potentially acts as an electrostatic catalyst through strengthening the hydrogen-bonding with the electron-deficient indole moiety.[64] As shown in Table 3, the calculated Mulliken charges of the proton, which forms a hydrogen bond with His55, become more positive in some intermediates and transition states in the proposed pathway. Indeed, geometry optimizations with the model M2 on intermediates ^{34} and ^{35} render the hydrogen bond

Table 3. Calculated Mulliken Charge of the Indole Proton Atom, Distance of Hydrogen Bond with His55, and Relative Energy Calculated by the ONIOM(B3LYP/BS1:MM) Method[a]

	M1			M2[b]	
	q_{H_N}	$r(H \cdots N_{his})$	ΔE_{ONIOM}	$r(H \cdots N_{his})$	ΔE_{ONIOM}
^{31}	0.34	1.92	4.7 (0.0)	1.92	(0.0)
$^3TS_{1-2}$	0.42	2.00	17.5		
^{32}	0.34	2.00	8.2 (3.5)		
$^3TS_{2-3}$	0.35	1.99	18.3		
^{33}	0.35	2.03	-16.4 (-21.1)	1.96	(-21.0)
$^3TS_{3-4}$	0.43	2.11	-8.9		
^{34}	0.45	2.09	-12.7 (-17.4)	1.82	(-23.8)
$^3TS_{4-5}$	0.36	1.97	-5.4		
^{35}	0.37	2.03	-23.1 (-27.7)	1.94	(-31.2)
$^3TS_{5-P}$	0.36	2.14	-18.5		

[a] The energies relative to ^{31} are given in parentheses. [b] Data obtained by using model M2.

stronger with His55, and thus enhance their stability (Table 3 and Figure S14). There was concern that formation of the proposed reactive ferryl-oxo intermediate would lead to side reactions,[15] but hydrogen-bonding should help lock the substrate to prevent side reactions, such as proton or hydrogen transfer to the oxo ligand[65] as well as oxo-attack to the benzene moiety of Trp.

3.7. Effects of Basis Sets, Functionals, QM Models, and Electronic Embedding. The effects of larger basis sets (BS2), B3LYP*, larger QM models (M3, M4), or polarization of the QM part by the electronic embedding (EE) scheme on the favorable pathway were examined (Table 2). In general, the energetic profile is not significantly changed by these factors, except that stability of intermediates and transition states (i.e., $^3TS_{3-4}$, ^{34}, $^3TS_{4-5}$, ^{35}, and $^3TS_{5-P}$) with the proton transferred to O_d were overestimated by ONIOM-ME with model M1. In these cases, electrostatic interactions with one 7-propionate side chain cannot be precisely described by ONIOM-ME with model M1, although the conclusion should not be changed. Therefore, by using ONIOM-EE or ONIOM-ME with M4, the calculated barrier for the acid-catalyzed ring-opening was suggested to be increased from 7 kcal/mol to about 10−13 kcal/mol; additionally, the stability of ^{34} is reduced by 10−14 kcal/mol (Table 2). However, a stable intermediate, ^{34}, with stronger hydrogen-bonding with the neutral amino of Trp ($O_dH \cdots N_{Trp} = 1.50$ Å, Figure S15) was obtained by ONIOM(B3LYP/BS1:MM)-ME optimization with model M4 with a higher stability ($\Delta E_{ONIOM} = -9.8$ kcal/mol). Therefore, the optimized energies for $^3TS_{3-4}$, ^{34}, $^3TS_{4-5}$, ^{35}, and $^3TS_{5-P}$ calculated by the ONIOM(B3LYP/BS1:MM)-ME method and small model M1 (columns 3−7 of Table 2) should be underestimated. Their stabilities, e.g. for ^{34}, should be enhanced by forming stronger hydrogen bonds with both the neutral amino of Trp and His55 (Figures S14 and S15, and Tables 2 and 3).

In summary, ONIOM calculations suggest an unusual mechanistic scenario of dioxygen activation and oxygenation in xcTDO (Scheme 8). Rather than the widely accepted electrophilic addition of the ferrous-dioxygen intermediate to C3 of the deprotonated indole part, the ferric-superoxide intermediate undergoes direct radical addition to C2 of the neutral indole part in the protein. Therefore, the proposed deprotonation of the indole part for electrophilic addition is not needed, since electron transfer from Fe(II) to the bound dioxygen gives the

(63) An asynchronic but concerted step was found in the first-step heme oxygenase: Chen, H.; Moreau, Y.; Derat, E.; Shaik, S. *J. Am. Chem. Soc.* **2008**, *130*, 1953.

(64) The water molecule was proposed to be an electrostatic catalyst in P450: Ahmet, A.; Guallar, V.; Friesner, R. A.; Shaik, S.; Thiel, W. *J. Am. Chem. Soc.* **2006**, *128*, 3924.

(65) Wang, Y.; Chen, H.; Makino, M.; Shiro, Y.; Nagano, S.; Asamizu, S.; Onaka, H.; Shaik, S. *J. Am. Chem. Soc.* **2009**, *131*, 6478.

Scheme 8. Our Proposed New Mechanism for xcTDO (Solid Arrows)[a]
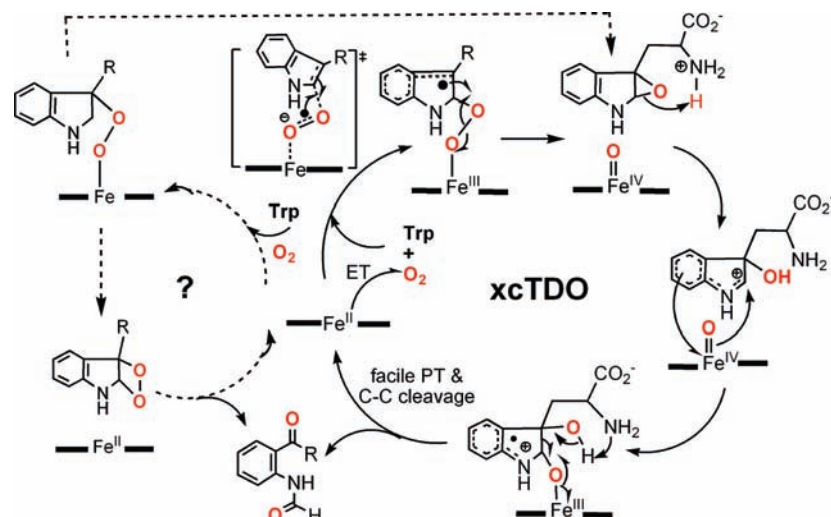
[a] The previously proposed feasible dioxetane route is also shown (dashed lines).

Scheme 9. Dioxygen Activation and Oxidation Process for Heme Systems
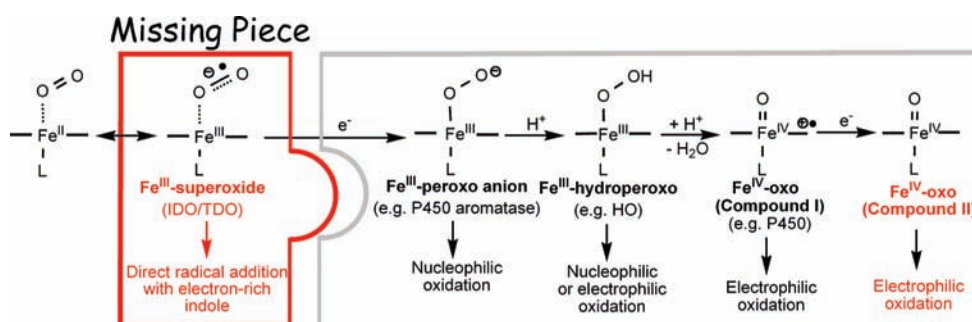
less-electrophilic ferric-superoxide intermediate as the oxidant.[15] The homolytic O−O bond-cleavage step then leads to the epoxide and ferryl-oxo intermediates. The metastable epoxide is found to be activated by proton transfer from the ammonium cation of the substrate itself for ring-opening and subsequent oxo-attack within the hydrophobic distal pocket. Finally, a low-barrier C−C bond cleavage and back proton transfer complete the catalytic cycle and afford *N*-formylkynurenine product.

During submission of this paper, the Hoffman and Raven groups observed the ferric-peroxy species of IDO and TDO in the absence and in the presence of the substrate and substrate analogue by cryoreduction/EPR/ENDOR techniques.[66] They deduced that the ammonium cation of the substrate forms a hydrogen bond with the Fe-bound dioxygen, which is consistent with [oss]1. In addition, the substrate or substrate analogue was found to exclude water in the active site and shield the cryogenerated ferric peroxy species from protonation. These results showed that residues in the active site do not act as a proton donor. In addition, decay of the cryoreduced peroxo-ferric species in the presence of the substrate or substrate analogue was found to occur only at high temperatures. A water molecule was suggested to diffuse into the active site during cryoreduction at high temperatures.[66] However, no water molecule can be found in the distal pocket in our 10-ns simulation. Alternatively, as shown in section 3.3, the am-

monium cation of the substrate, which should also form a hydrogen bond with the ferric-peroxy species, can potentially act as the sole proton donor.

This atom-economic[67] oxygenation reaction in TDO does not use external electrons and protons, but the redox ferrous heme acts as a temporary electron donor during the reaction, and the substrate provides overall four electrons and a proton source. Such a tactic for dioxygen activation and oxygenation of the substrate via dual oxidants (ferric-superoxide and ferryl-oxo intermediates) in xcTDO is rather unique in heme systems (Scheme 9). The hydrophobic distal pocket as well as the absence of a hydrogen-bond network and external reductant[6a,8] in xcTDO should be critical for the first mild oxidant, ferric-superoxide intermediate to selectively incorporate the first oxygen atom with the reactive indole of Trp, as well as protect the ferryl-oxo (Cpd II) intermediate for the second oxygen atom incorporation.

We could envision that the fate of the final oxygenation product could be changed by supplementing external electron or/and proton transfer as in the other heme oxygenases (Scheme 9). For instance, the ferric-peroxy intermediate is proposed as the oxidant for aromatase.[1e,3d,51e,68] Increasing nucleophilicity for the peroxy anion results in an increased barrier for addition with the electron-rich indole[15,66] and enhanced proton affinity to accept one proton (e.g., from the bulk phase or nearby

(66) Davydov, R. M.; Chauhan, N.; Thackray, S. J.; Ross Anderson, J. L.; Papadopoulou, N. D.; Mowat, C. G.; Chapman, S. K.; Raven, E. L.; Hoffman, B. M. *J. Am. Chem. Soc.* **2010**, *132*, 5494.

(67) Trost, B. M. *Science* **1991**, *254*, 1471.
(68) Wertz, D. L.; Valentine, J. S. In *Structure & Bonding*; Meunier, B., Ed.; Springer-Verlag: Berlin, 2000; Vol. 97, pp 37−60.

Table 4. Calculated Mössbauer Parameters of the Key Intermediates[a] for xcTDO at the B3LYP/BS3 Level in the Presence of the MM Fixed Point Charges Based on the ONIOM(B3LYP/BS1:Amber) Optimized Structures

	V_{zz}	V_{xx}	V_{yy}	η	ΔE_Q (mm/s)	δ_{Fe} (mm/s)
css**1**	1.43	−0.41	−1.02	0.43	−2.39	0.31
oss**1**	1.40	−0.41	−0.99	0.42	−2.33	0.62
31	1.60	−0.26	−1.34	0.67	−2.78	0.42
oss**2**	1.37	−0.17	−1.20	0.76	−2.42	0.38
32	1.37	−0.16	−1.20	0.76	−2.42	0.37
33	−1.10	0.49	0.61	0.11	1.78	0.08
35	1.46	−0.23	−1.23	0.69	−2.54	0.40

[a] Data obtained by using model M1 in these calculations.

ammonium cation) to give the ferric-hydroperoxy intermediate. The ferric-hydroperoxy intermediate, the key intermediate for HO and NOS,[1e,3a,b,51a−d,52,63] can undergo homolytic O−O bond cleavage to give a reactive hydroxyl radical, which could possibly react with the indole, followed by oxo-attack to give the *cis*-dihydroxylation product, or could react with the *meso* carbon (the first-step heme degradation). Alternatively, the ferric-hydroperoxy intermediate, analogous to the first oxygenation step of NOS,[52d−f] could accept one proton (e.g., from the ammonium cation) to give the reactive ferryl-oxo (Cpd I) intermediate and one water molecule. As a result, external electron and proton transfer could alter the function of the heme to become a heme monooxygenase (e.g., epoxidation of the indole or oxygenation of the amino group[52e,f]). Therefore, the involvement of the proposed dual oxidants and exclusion of external electron and proton transfer are the keys for a heme dioxygenase with Trp substrate. On the other hand, some non-heme dioxygenases adopt different strategies for oxygenation.[3c,e,k] Unlike the common six-coordinate oxy-heme intermediate, a coordinately unsaturated/flexible non-heme center can further activate the substrate through ligation (as well as deprotonation) or/and the bound dioxygen or hydroperoxy through a side-on coordination mode. For the non-heme ferric-hydroperoxy intermediate, a reactive O=Fe(OH) intermediate could then be transformed for epoxidation or *cis*-dihydroxylation (2e oxidation in both cases).[69] Moreover, some non-heme dioxygenases (e.g., α-keto acid-dependent enzymes and pterin-dependent aromatic amino acid hydroxylases) utilize the reactive cofactor to react with the mild ferric-superoxide species followed by O−O bond cleavage to generate the reactive ferryl-oxo species, which then oxidizes the substrate. In this case, one oxygen atom is incorporated to the cofactor, and the other oxygen atom is incorporated to the substrate.

3.8. Mössbauer Parameters. Since Mössbauer spectroscopy is an important tool to characterize intermediates in iron-containing complexes,[70] the quadrupole splitting and isomer shift of stable intermediates in Scheme 8 were estimated by the ONIOM(B3LYP/BS3:MM)-EE//ONIOM(B3LYP/BS1:MM)-ME method (Table 4). Distinct from the intermediates containing an Fe(II) or Fe(III) center, the ferryl-oxo (Cpd II) intermediate

(69) (a) Bukowski, M. R.; Comba, P.; Lienke, A.; Limberg, C.; Lopez de Laorden, C.; Mas-Ballesté, R.; Merz, M.; Que, L., Jr. *Angew. Chem., Int. Ed.* **2006**, *45*, 3446. (b) Bassan, A.; Blomberg, M. R. A.; Siegbahn, P. E. M.; Que, L., Jr. *Angew. Chem., Int. Ed.* **2005**, *44*, 2939. (c) Quiñonero, D.; Morokuma, K.; Musaev, D. G.; Mas-Balleste, R.; Que, L., Jr. *J. Am. Chem. Soc.* **2005**, *127*, 6548.
(70) (a) de Oliveira, F. T.; Chanda, A.; Banerjee, D.; Shan, X.; Mondal, S.; Que, L., Jr.; Bominaar, E. L.; Münck, E.; Collins, T. J. *Science* **2007**, *315*, 835. (b) Bukowski, M. R.; Koehntop, K. D.; Stubna, A.; Bominaar, E. L.; Halfen, J. A.; Münck, E.; Nam, W.; Que, L., Jr. *Science* **2005**, *310*, 1000.

Table 5. Calculated Relative Energy (kcal/mol) of the Direct Radical Transition State ($\Delta E^{\ddagger}$) and Product (ΔE) for Various Substrates at the B3LYP/BS1 Level in the Gas Phase

substrate	$\Delta E^{\ddagger\ a}$	ΔE^a
3-Me-indole	9.1[b]	−0.2[b]
CH_2CHMe	13.3[c]	0.1
$CH_2CMeCHCH_2$	8.4	−11.3
C_6H_6	20.2	13.0
$C_6H_6O^-$	0.2	−15.1
pyrrole	8.5	1.0

[a] Energy of the transition state or product is relative to the isolated low-spin Fe^{II}-porphine, O_2, and the substrate. [b] Data from ref 15. [c] Relative energy for hydrogen abstraction from the methyl group (first-step hydroxylation) is 20.2 kcal/mol. The kinetic preference toward the addition over the hydrogen abstraction is reduced to 3.9 kcal/mol when zero-point energy correction is included.

33 has a positive quadrupole splitting (1.78 mm/s) as well as the lowest isomer shift (0.08 mm/s). These parameters (ΔE_Q and δ_{Fe}) for Cpd II in xcTDO are quite similar to those in other hemes (e.g., 1.44 and 0.09 in myoglobin, 1.59 and 0.11 in CPO, as well as 1.61 and 0.03 mm/s in horseradish peroxidase, respectively).[62c] Therefore, the calculated Mössbauer parameters for xcTDO may be useful to observe the proposed and as-yet-uncharacterized intermediates, particularly Cpd II, in future experiments.

3.9. Active-Site Model. To further understand the role of the protein, we removed the MM protein part and carried out optimization with model M1 in the gas phase. The favorable reaction pathway found in the protein (Scheme 8) was also found in these active-site model calculations (Figure S17), despite some differences in energetic profiles and structures. For instance, in the absence of His55, the indole NH can form a hydrogen bond with the oxo ligand or interact with the porphine ring. On the other hand, the ammonium cation of Trp freely moves above and forms a stronger hydrogen bond (1.668 Å) with the O_d in the ferric-superoxide intermediate **3**I, which presumably increases the reaction barriers for the direct radical addition at C2 ($\Delta E^{\ddagger}_{ZPE} = 18.6$ kcal/mol) as well as the homolytic O−O cleavage coupled with epoxidation ($\Delta E^{\ddagger}_{ZPE} = 24.0$ kcal/mol). In addition, the ammonium cation forms a stronger hydrogen bond with the oxo ligand but a weaker hydrogen bond with the epoxide oxygen in **3**III. That increases the reaction barrier for the ring-opening. The overall active-site model results suggested that the protein confines the substrate, O_2, and heme in the preorganized and active conformation for the whole oxygenation process,[6b] which reduces the reaction barriers and avoids side reactions.

3.10. Direct Radical Addition of Ferric Superoxide Heme Species with Other π-Substrates. The proposed dioxygen activation and oxygenation via the radical reaction with the ferric-superoxide heme intermediate in xcTDO is quite unique in heme-containing oxygenases (Scheme 9).[1e,3a,b,d,f,g,49] Hence, it is interesting to explore the possibility of the proposed radical addition with other small π-systems as representatives (Table 5 and Figure S18). Based on the active-site model calculations, we are pleased to show that the relative energy of the direct radical addition transition state for ferric-superoxide porphyrin intermediate with propene, 2-methylbutadiene, phenoxide anion, or pyrrole is similar to or lower than that for 3-methylindole (the simplified model for Trp).[71] Consequently, these theoretical

(71) A very small additional imaginary frequency was found for the addition TS for PhO⁻ (12.9*i* cm⁻¹) and the addition product for the diene (2.9*i* cm⁻¹).

results imply that *reaction of the not-well-recognized ferric-superoxide heme intermediate as the oxidant, which is less reactive than Cpd I and Cpd II oxidants, with other π-systems or even other reactive systems*[49] *might take place in the hemes*, provided that both electron and proton transfer to the ferric-superoxide heme intermediate are suppressed and the substrate is oriented conveniently for the oxygenation.[6b]

4. Conclusions

Unique TDO and IDO can catalyze oxidative cleavage of the pyrrole ring of L-tryptophan (Trp). Although these two heme dioxygenases were discovered more than 40 years ago, their reaction mechanisms have remained poorly understood. In this study, ONIOM(B3LYP:Amber) calculations do not support the recently proposed mechanisms for xcTDO (via either formation of the dioxetane intermediate or Criegee-type rearrangement) but suggest a rather unique mechanism in the hemes: (1) direct radical addition of a ferric-superoxide intermediate with C2 of the indole of Trp, followed by (2) ring-closure via homolytic O−O cleavage to give epoxide and ferryl-oxo (Cpd II) intermediates, (3) acid-catalyzed regiospecific ring-opening of the epoxide, (4) oxo-coupled electron transfer, and (5) finally C−C bond cleavage concerted with back proton transfer (Scheme 8). The computed barrier for the first oxygen incorporation is about 17−19 kcal/mol, while the estimated barrier for the second oxygen incorporation is more than 10 kcal/mol but less than 20 kcal/mol. More reliable QM/MM free energy calculations will be performed and reported in due course. Our calculations propose that the involvement of dual oxidants, ferric-superoxide and ferryl-oxo (Cpd II) intermediates, is important for the dioxygenase reactivity in xcTDO. Moreover, the not-well-recognized ferric-superoxide porphyrin intermediate is suggested to be a potential oxidant with some π-systems via direct radical addition in the hemes. Interestingly, two competitive pathways (via direct electrophilic/radical addition with C2 or C3 positions of the indole followed by formation of the dioxetane or ferryl-oxo intermediates) were previously proposed to operate in the gas-phase active-site model.[15] On the other hand, xcTDO is suggested to choose one of the pathways (i.e.,

direct radical addition followed by the formation of the ferryl-oxo intermediate). The proposed mechanism for xcTDO might also operate in other TDO or IDO, if the substrate binding in these proteins is very similar. It should be noted that the ferryl-oxo (Cpd II) species has just been observed in hIDO, but not in hTDO.[17a,b] Moreover, *N*-formylkynurenine is formed when the assumed ferryl-oxo species in hIDO is present; therefore, the ferryl-oxo might be an intermediate in the catalytic cycle.[17a] These results also suggest either a shorter lifetime of the ferryl-oxo species, if transiently formed, or another operating mechanism in hTDO.[17b] If Trp is mobile to have multiple binding modes in the ternary complex[17b,72] and O_d could readily access C3 of Trp, the possibility of the proposed competitive mechanism via direct radical addition to C3 followed by formation of a dioxetane intermediate[15] (Scheme 8) might be good. Overall mechanistic pathways for the old TDO bring us more new knowledge of the heme chemistry. More experimental studies[17a,b,50] are called for, characterizing the proposed intermediates.

Supporting Information Available: Complete refs 6a, 21, and 44; Cartesian coordinates for the QM calculations; absolute energies; Figures S1−S18; Scheme S1; Tables S1−S8; and Movies S1−S5. This material is available free of charge via the Internet at http://pubs.acs.org.

JA103530V

(72) Macchiarulo, A.; Nuti, R.; Bellocchi, D.; Camaioni, E.; Pellicciari, R. *BBA-Proteins Proteom.* **2007**, *1774*, 1058.